(This is a sample cover image for this issue. The actual cover is not yet available at this time.)

Science of the Total Environment 432 (2012) 65–77

Contents lists available at SciVerse ScienceDirect

Science of the Total Environment

journal homepage: www.elsevier.com/locate/scitotenv

Dust-mediated loading of trace and major elements to Wasatch Mountain snowpack

Gregory T. Carling, Diego P. Fernandez, William P. Johnson *

University of Utah, Dept. of Geology & Geophysics, Salt Lake City, UT, USA

ARTICLE INFO

Article history:
Received 26 October 2011
Received in revised form 7 May 2012
Accepted 14 May 2012
Available online xxxx

Keywords:
Aeolian dust
Trace elements
Mercury
Snow chemistry
Dust chemistry
Wasatch Mountains

ABSTRACT

Depth-integrated snow columns were collected at 12 sites across the central Wasatch Mountains, Utah, during March and April 2010 to determine concentrations of trace elements, major anions and cations, and pH. Sample collection was conducted at or near maximum snow accumulation prior to the onset of melt, and included spring dust events driven by southerly pre-frontal winds. Snow samples were melted in the laboratory and subsampled for analyses on filtered (0.45 μm) and unfiltered fractions. All measured elements (Al, As, Ba, Ca, Co, Cr, Cu, Fe, Hg, K, Li, Mg, Mn, Na, Ni, Pb, Sb, Sr, Ti, Tl, U, V, and Zn) and major anions (Cl, NO_3, and SO_4) displayed significant increases in concentration (for example, factor of 2 to 5 increases for As, Cr, Hg, and Pb) between the six sites sampled in March (prior to dust events) and the six sites sampled in April (after dust events). Acid neutralizing capacity and pH were also elevated in April relative to March snowpack. Comparison of elemental concentration in the particulate (>0.45 μm; difference between unfiltered and filtered concentration) and soluble (<0.45 μm; filtered concentration) fractions shows that the concentration increase between March and April snowpack for the trace elements is primarily a result of association with dust particles >0.45 μm. The results suggest that the majority of trace element loading to the Wasatch snowpack occurs via dust deposition. The major elements were primarily loaded in the <0.45 μm fraction, suggesting deposition of soluble dust particles. The overall findings of this paper are similar to other studies regarding the role of dust on nutrient and trace element accumulation in soils and lake sediments, but to our knowledge this is the first study that compares trace element chemistry of seasonal snowpack before and after dust deposition events.

1. Introduction

Aeolian (wind-blown) dust is an important source of trace and major elements to snowpack worldwide, as shown in ice core records from polar, mid-latitude, and tropical glaciers (Correia et al., 2003; Ferrari et al., 2001; Hong et al., 2004a,b, 2005, 2009; Marteel et al., 2009; Thevenon et al., 2011). Dust contributes both soluble and insoluble mineral particles to snowpack, leading to differences in the fate and transport of associated elements during snow melt runoff (Bacardit and Camarero, 2010; Gaspari et al., 2006; Grotti et al., 2011). In addition to dust, other sources of element loading to snowpack include anthropogenic emissions, sea salt spray, and volcanic tephra (Ayling and McGowan, 2006; Gabrielli et al., 2008; Veysseyre et al., 2001). In the seasonal snowpack of mid-latitude mountain ranges, major ion concentrations have been well-documented through comprehensive sampling campaigns (e.g. Clow et al., 2002; Laird et al., 1986; Turk et al., 2001; Winiwarter et al., 1998); whereas trace element concentrations in seasonal mid-latitude snowpack have only been examined in a limited number of investigations (Bacardit and Camarero, 2010; Fortner et al., 2009; Gabrieli et al., 2011; Gabrielli et al., 2008; Kang et al., 2007; Lee et al., 2008; Veysseyre et al., 2001). In the above studies, the correlation between trace and major elements with dust particles is well established either through measurements of dust properties or by statistical methods. Furthermore, two recent studies (Rhoades et al., 2010 and Lawrence et al., 2010) have reported elevated major ion concentrations in snowpack that contained visible dust layers relative to dust-free snowpack. However, neither of these studies, nor others in the literature, have provided data on trace element concentrations in seasonal snowpack with and without visible dust layers. Furthermore, no previous studies have reported trace element concentrations in Wasatch Mountain snowpack.

The Wasatch Mountains, with 1–2 km vertical relief and a unique geographic location, situated downwind of both the Wasatch Front urban area (including the Salt Lake Valley) and the Great Basin desert, potentially act as a catchment barrier for atmospheric deposition of trace and major elements from dust and anthropogenic sources (Fig. 1). Furthermore, Wasatch snowmelt is a major source of water for the expanding population along the Wasatch Front which now exceeds 2 million people (Price, 1985). The Wasatch Front urban area is meteorologically up-gradient and hydrologically down-gradient from the Wasatch Mountains. No other major urban center in the U.S. is located so close (<25 km from the urban center to alpine snowpack) and in this arrangement to its water source.

* Corresponding author at: 115 S 1460 E Rm 383, Salt Lake City, UT 84112-0102, USA. Tel.: +1 801 581 5033.
E-mail address: william.johnson@utah.edu (W.P. Johnson).

0048-9697/$ – see front matter © 2012 Elsevier B.V. All rights reserved.
doi:10.1016/j.scitotenv.2012.05.077

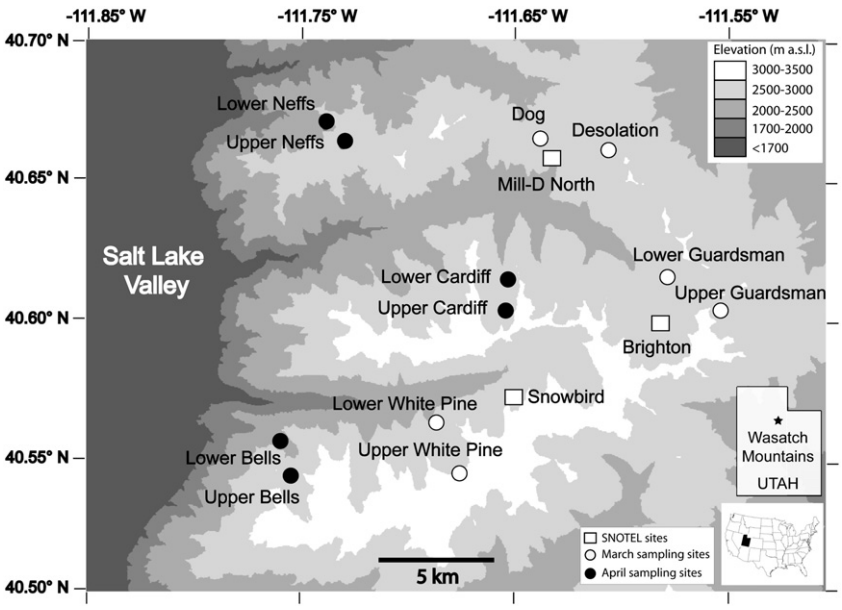

Fig. 1. Location of sampling sites and SNOTEL sites in the central Wasatch Mountains, Utah. Depth-integrated snow columns were collected during March or April at each sampling location. Essentially all area <1700 m a.s.l. elevation is part of the urbanized Salt Lake Valley.

Numerous anthropogenic and natural contaminant sources are located upwind of the Wasatch Mountains. The buildup of anthropogenic pollution and particulate matter during winter temperature inversions in the Salt Lake Valley has been implicated as a local source of trace and major elements to the Wasatch snowpack. For example, Cerling and Alexander (1987) observed elevated major ion concentrations in Wasatch snow collected during an inversion period. The Great Basin desert of Nevada and western Utah, which is characterized by alternating mountains and arid playa basins, is a regional source of dust and associated contaminants. Neff et al. (2008) showed that aeolian dust deposition to the western U.S. has increased beginning in the 20th century due primarily to land use changes. It is possible that wind-blown dust events in the Great Basin desert will increase in frequency and intensity due to climate change (Munson et al., 2011), increasing groundwater extraction, population growth, and expanding desert land disturbance. Dust has been shown to have a profound effect on the radiation balance of snowpack in the Colorado Rockies, leading to earlier snowmelt and decreased runoff (Painter et al., 2007, 2010). Furthermore, aeolian dust has been shown to affect landscape geochemistry, ecology, lakebed sediment chemistry, and surface water and groundwater chemistry in the western U.S. (Goldstein et al., 2008; Lawrence et al., 2010; Mayo and Klauk, 1991; Reynolds et al., 2010).

The objectives of this paper are to examine trace and major elements in snowpack that reflect a range of sources from anthropogenic to natural, describe partitioning of elements between the soluble and particulate (insoluble) fractions, and compare Wasatch snow chemistry to that of other mid-latitude locations. Given the proximity of the Wasatch Mountains to a major metropolitan area, as well as influence of dust storms from the arid Great Basin, we hypothesized that Wasatch snowpack would contain elevated levels of trace and major elements relative to other mountain ranges. To investigate Wasatch snowpack chemistry and pathways of element deposition, we collected depth-integrated spring snowpack profiles across the Wasatch Mountains before and after dust deposition events. Additionally, we isolated dust layers from the snowpack to make direct measurements of dust chemistry. Pre-dust snow samples represent ambient wintertime wet and dry deposition, whereas snow samples with visible dust layers capture the springtime flux of aeolian dust and associated elements. This paper shows the effect that spring dust storms have on the chemistry of winter-accumulated snowpack during a single year; however, this paper does not attempt to provide an annual budget of dust fluxes to the Wasatch Mountains (which is variable year to year). Dust events in the Great Basin are most common during late winter to early spring (Steenburgh et al., in press), when elevated wind speeds are most frequently observed (Jewell and Nicoll, 2011), coinciding to the time period of maximum snowpack accumulation. Thus the monitoring time frame (collection of snowpack at or near maximum accumulation prior to the onset of melt) is comprehensive with respect to snowpack chemistry as it spans the time period of snow exposure to material transport from the urban Salt Lake Valley and the Great Basin desert.

2. Material and methods

2.1. Sample collection

Depth-integrated snow columns were collected at 12 sites in the Wasatch Mountains between 18 March and 17 April 2010 (Fig. 1 and Table 1) at or near maximum snow accumulation prior to the onset of melt. The study area is hereby referred to as the "central Wasatch". Snow was collected from sites which met the following criteria: 1) flat, wind-protected area; 2) clearing within or adjacent to coniferous/deciduous forests; 3) beyond canopy drip edge and likewise not affected by through fall; 4) minimal impact from recreationists, including snowmobiles; 5) no avalanche debris; 6) >0.5 km from ski resort boundaries or roads; and 7) no local impact from avalanche artillery. Sampling locations were accessed using skis or snowshoes.

The central Wasatch had substantial (>50 cm) snow cover beginning 13 December 2009 and received continued accumulation until sampling was completed on 17 April 2010 (Supporting Information Fig. S1). Thus the collected snow columns represent the entire winter snowpack from mid-December 2009 until the date of sample collection during the final month of snow accumulation (between 18 March and 17 April 2010). The snow samples provide an archive of bulk (wet and dry) deposition of trace and major elements across the winter and spring, or the entire annual accumulation period. The snowpack was warming throughout the sampling period, as indicated by isothermal/near-isothermal conditions measured in snow pits. However, full scale melt did not begin until

Table 1
Details of sample collection and snowpit measurements for snow sampling campaign across the central Wasatch Mountains.

Snow pit location	Sampling date	Latitude (°N)	Longitude (°W)	Elevation (m)	Depth of sampled snow profile (cm)	Total snow depth (cm)	SWE (cm)	# of samples from each snow pit
								Snow column/bottle scrape
Desolation	3/18/2010	40.662	111.606	2822	120	156	30.31	2/0
Dog	3/18/2010	40.666	111.638	2682	90	121	36.81	2/0
Upper White Pine	3/25/2010	40.546	111.675	2931	145	180	50.88	1/1
Lower White Pine	3/25/2010	40.564	111.686	2644	120	148	58.60	2/1
Upper Guardsman	3/27/2010	40.604	111.553	2880	156	206	53.04	2/0
Lower Guardsman	3/27/2010	40.616	111.578	2669	112	130	39.85	2/0
Upper Neffs	4/3/2010	40.664	111.730	2713	210	235	65.32	1/1
Lower Neffs	4/3/2010	40.671	111.738	2473	129	163	51.12	2/0
Upper Bells	4/10/2010	40.544	111.753	2743	250	299	92.88	1/1
Lower Bells	4/10/2010	40.557	111.759	2335	140	180	53.81	2/0
Upper Cardiff	4/15/2010	40.604	111.653	2816	211	259	77.94	1/1
Lower Cardiff	4/15/2010	40.615	111.653	2576	146	186	61.41	2/0
Desolation (Dec–March re-sample)	4/17/2010	40.662	111.606	2822	89	130	26.07	2/0
Desolation (April snow only)	4/17/2010	40.662	111.606	2822	77	77	24.89	2/0
Dog (Dec–March re-sample)	4/17/2010	40.666	111.638	2682	60	102	41.22	2/0
Dog (April snow only)	4/17/2010	40.666	111.638	2682	47	47	17.70	2/0

after sampling was complete as indicated by soil moisture and air temperature data measured at National Resource Conservation Service snow telemetry (SNOTEL) sites located within the study area (Supporting Information Figs. S2 and S3; SNOTEL data further described in Section 2.6), as well as by the similarity of results for snowpack sampled in March and then re-sampled during April (discussed in Section 3.3).

The original goal of our sampling scheme was to compare the spatial variability in snowpack chemistry across the central Wasatch. However, it became apparent that temporal variability in snowpack characteristics during the sampling period was more important than spatial variability (as described in Section 4.1). The temporal change was due to the deposition of dust and additional snow beginning halfway through the sampling period: dust layers were deposited on 30 March, 5 April, and 11–12 April 2010 (Fig. 2), and the individual dust events were followed by snow accumulation totaling ~20 cm snow water equivalent (SWE) measured at SNOTEL stations and snow pits between 30 March and 17 April (Fig. 3). Thus the six locations sampled prior to 30 March contain a record of ambient seasonal snowpack conditions without visible dust, whereas the six locations sampled after 30 March contain a record of seasonal snowpack plus spring-accumulated dust and snow (Table 1).

At each site, a snow pit was excavated to within 10 cm of the ground. Observations regarding snowpack features were recorded, including total snowpack depth, snow temperature in 10 cm increments (Turk et al., 2001), presence of visible dust layers (Lawrence et al., 2010), and presence of liquid water between snow grains. Cores were collected behind the snow pit face using a clean acrylic tube (5.08 cm inside diameter, 50 cm length) that was transported to the sample site in plastic wrap. The acrylic tube was cleaned by soaking in 10% HCl for 2–3 days, rinsing multiple times with Milli-Q water, and drying in a laminar flow hood. In order to minimize potential contamination from soil and plant material, and to exclude snow that accumulated prior to December, the bottom 18–50 cm (mean: 36 ± 10 cm) of snow from each snow pit was not collected (Table 1). Therefore, concentrations represent an average of between 74 and 89% (mean: $80 \pm 5\%$) of the entire snow column. Although not sampling the entire snow depth may lead to errors in calculating the seasonal snow budget and element loads, we decided to take a conservative approach by excluding all snow that was not representative of the overall snowpack such as early season (pre-December) faceted snow near the ground.

The individual cores (i.e. 50 cm subsections) were composited in a double-bagged clean 2.5 L FLPE bottle to obtain a depth-integrated snow column sample. The 2.5 L FLPE bottles were acid washed, rinsed, and dried using the same procedure described above for the acrylic tubes. Snow samples were kept frozen during transport to the laboratory, where samples were stored in a freezer at −20 °C until further processing. Clean hands, dirty hands" protocols (USEPA, 1996) were followed in all steps of the sampling process, and operators wore new powder-free vinyl gloves and non-fibrous clothing. To assess potential contamination by sampling and processing methods, a field blank was collected on 17 April by pouring 1 L Milli-Q water through a clean acrylic tube into an empty 2.5 L FLPE bottle while the operators stood in an excavated snow pit. The field blank was collected on the final day of sampling, after dust deposition events, and thus is likely to contain maximum background concentrations of all elements due to accumulation of

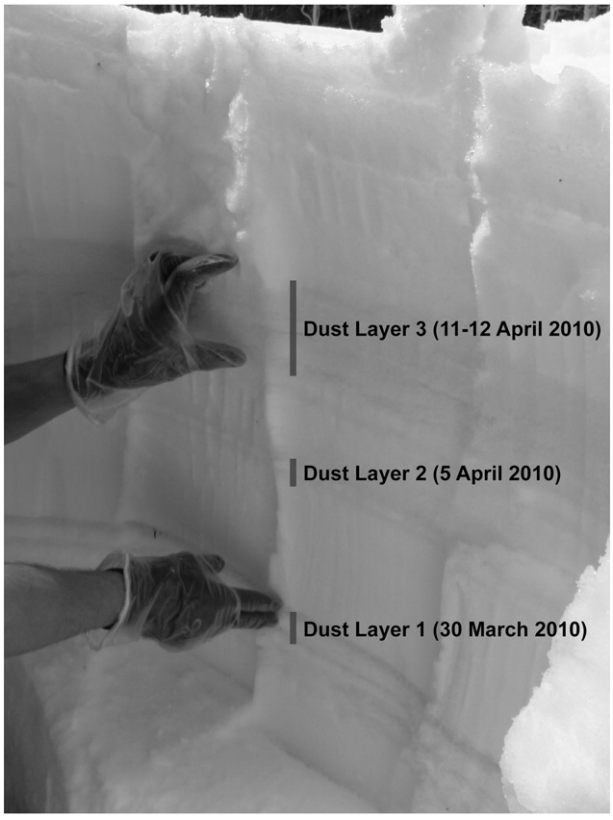

Fig. 2. Photograph showing dust layers deposited across the central Wasatch on 30 March, 5 April, and 11–12 April 2010.

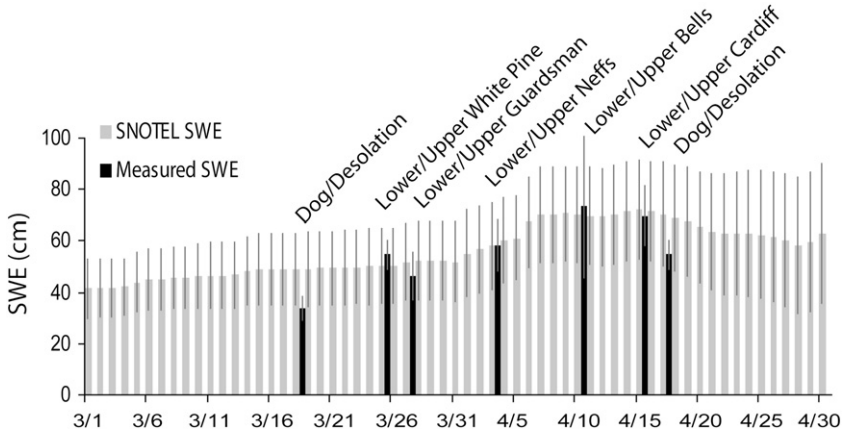

Fig. 3. Daily average snow water equivalent (SWE) measured at three SNOTEL sites ("SNOTEL SWE") and two snow pits ("Measured SWE"). Error bars represent ±1 s.d.

snow and dust in the snow pit. The field blank was stored, thawed, subsampled, filtered, and acidified using the same procedures described in Section 2.2 for snow column samples. In addition to the field blank, a laboratory blank was prepared to test background contamination from sample bottles, reagents, and the laboratory environment. For the laboratory blank, 1 L Milli-Q water was poured into an empty 2.5 L FLPE bottle and immediately subsampled and acidified for analyses. Results for the field blank and laboratory blank samples are shown in the Supporting Information (Table S1) and described in Section 2.4.

On each sampling day (three sampling days in March, prior to dust deposition, and three sampling days in April), snow pits were excavated at a paired upper elevation (>2700 m a.s.l.) and lower elevation (<2700 m a.s.l.) site (for a total of 12 snow pits). Details of sample collection, sampling locations, and snowpack characteristics are provided in Table 1. The following locations were sampled (see Fig. 1 and Table 1): 1) Desolation and Dog on 18 March; 2) Upper and Lower White Pine on 25 March; 3) Upper and Lower Guardsman on 27 March; 4) Upper and Lower Neffs on 3 April; 5) Upper and Lower Bells on 10 April; and 6) Upper and Lower Cardiff on 15 April. The average elevation of all sampling sites is 2690 ± 170 m a.s.l.

Two depth-integrated snow samples were collected from each snow pit (1–2 m apart), either as duplicate snow column samples (at 8 sites) or as one snow column and one "bottle scrape" sample (at 4 sites) (Table 1). The bottle scrape samples were collected by scraping the wide-mouth 2.5 L FLPE bottle vertically across a clean section of the snow pit wall, applying even pressure in order to collect all snow layers in equal proportion. Additionally, at the Lower White Pine site two snow column samples and one bottle scrape sample were collected to provide further comparison between the two collection methods. The two collection methods provided similar results (Supporting Information Table S2), with concentrations of most elements agreeing within ±0–25% between snow column and bottle scrape samples, which is equivalent to the agreement between duplicate snow column samples.

Due to the substantial accumulation of snow and dust during the study period (described above), the Dog and Desolation sites were re-visited (to within 50 to 100 m of original sampling locations) on 17 April (Table 1) to examine the influence of dust. Separate snow columns were collected below the lowest dust layer (to isolate snow that accumulated prior to 30 March) and above (to isolate snow and dust that accumulated 30 March and beyond) in order to provide a direct comparison of elemental composition of pre- and post-dust snowpack. Other sites besides Dog and Desolation were not re-visited because successive warm days after 17 April (with minimum air temperatures above 0 °C; Supporting Information Fig. S3) led to widespread snow melt across the central Wasatch; thus the snowpack stratigraphy likely would not have been preserved sufficiently to compare April versus March snowpack.

2.2. Sample preparation

Snow samples were thawed in a refrigerator at 4 °C for ~5 days within 1 month of collection in the same double bagged closed container in which they were collected. Water volume was measured gravimetrically to convert snow column volume to SWE. Melted snow was subsampled for bulk analyses of Hg (~200 mL), trace elements and major cations (60 mL), and pH/acid neutralizing capacity (ANC) (~200 mL). Additionally, 150 mL of melt water was filtered by forcing water through 0.45 μm clean PES syringe filters using clean 60 mL plastic syringes. Syringe filters were cleaned by forcing 50 mL of 10% v/v HCl through the filter membrane, followed by rinsing with 150 mL of Milli-Q water, and syringes were filled with 10% v/v HCl, double-bagged, placed in an oven at 60 °C for 2–3 days, triple rinsed with Milli-Q water, and dried in a laminar flow hood. Splits of filtered melt water were subsampled for analyses of Hg, trace elements/major cations, and major anions. Subsamples for Hg and trace element/major cation analyses were transferred to clean FLPE and LDPE bottles and preserved with 1% v/v BrCl and 2.4% v/v HNO_3, respectively. Other major ion subsamples (pH/ANC and anions) were transferred to clean HDPE bottles and immediately re-frozen. Additionally, 10 snow samples were sub-sampled for methyl Hg (MeHg) analysis (transferred to clean FLPE bottles and preserved with 1% v/v HCl). LDPE bottles were cleaned following the same procedures described above for syringes, whereas HDPE bottles and FLPE bottles (for Hg and MeHg subsamples) were cleaned by triple rinsing with Milli-Q water and drying in a laminar flow hood.

Sine our objective was to measure environmentally accessible trace and major elements, particles contained in the snowmelt were not digested prior to analysis. Melted snow samples for Hg and trace element/major cation analyses were prepared using a minimal acid concentration necessary for preserving routine aqueous samples in order to provide an estimate of the elemental fraction available to affect snowmelt runoff. This extraction method (acidification with 2.4% v/v HNO_3) is similar to that of Gabrielli et al. (2008) and Kang et al. (2007), who respectively used 2% and 1% HNO_3, but arguably less aggressive than the method used by Bacardit and Camarero (2010), who extracted the particulate fraction by dissolving filters in concentrated HNO_3 and H_2O_2 at 95 °C, and acidified the filtered fraction with 1% v/v HNO_3.

2.3. Sample analyses

Hg and MeHg subsamples were analyzed within 3 and 6 months, respectively, of sample collection using a Brooks Rand Model III CVAFS. Hg and MeHg concentrations were determined according to EPA Methods 1631e (USEPA, 2002) and 1630 (USEPA, 2001), respectively. At a minimum, matrix spike recoveries and replicates were analyzed for every 10 samples. For the sample run to be accepted, matrix spike recoveries had to fall within 75–125% of the original sample run and replicate analyses had to fall within ±10%. Method blanks were analyzed at the beginning of each run in order to calculate a detection limit (D.L.). The accepted D.L. is 0.4 ng/L and 0.02 ng/L for Hg and MeHg, respectively.

Trace element/major cation subsamples were analyzed within 3 months of sample collection using a quadrupole inductively coupled plasma mass spectrometer (ICP-MS) with a collision cell (Agilent 7500ce) to measure concentrations of Ag, Al, As, Ba, Be, Ca, Cd, Co, Cr, Cu, Fe, K, Li, Mg, Mn, Mo, Na, Ni, Pb, Sb, Se, Sr, Ti, Tl, U, V, and Zn. A double-pass spray chamber with perfluoroalcoxy fluorocarbon (PFA) nebulizer (0.1 mL/min), a quartz torch and platinum cones were used. A calibration solution containing all the elements reported was prepared gravimetrically using 1000 mg/L single-element standards (Inorganic Ventures, Inc.). This solution was used to prepare a calibration curve with six points plus a blank. Ca, Cr, Fe, K, Mn, Na, and V were determined using 4 mL He/min in the collision cell, and As and Se were determined using 4 mL He/min plus 2.5 mL H_2/min. D.L. was determined as three times the standard deviation of the 23 blanks analyzed throughout the run. A USGS standard reference sample (T-205), diluted 1:4, was analyzed ten times together with the samples as a continuing calibration verification. The long term reproducibility for T-205 and differences relative to the accepted values obtained using our method indicate that the elemental concentrations reported here are accurate within 10% for most elements (Supporting Information Table S3).

ANC and pH were measured on unfiltered samples (as performed by Turk et al., 2001) using a Mettler Toledo DL50 v2.4 titrator with 1:5000 M HCl and Oakton 1100 series pH meter, respectively. Major anions (Cl^-, NO_3^-, and SO_4^{2-}) were measured on filtered samples using a Dionex 4100 ion chromatograph (IC).

2.4. Data analysis and quality control

Major ion charge balances were calculated using cation concentrations (Ca^{2+}, Mg^{2+}, Na^+, and K^+) from filtered ICP-MS subsamples, anion concentrations (Cl^-, NO_3^-, and SO_4^{2-}) from filtered IC subsamples, and ANC concentrations (which was assumed to be comprised of HCO_3^-). Some of the Dec–March (pre-dust) samples showed evidence for Ca^{2+} contamination in the filtered fraction (where measured filtered concentration ≫ unfiltered concentration); therefore, unfiltered Ca^{2+} concentrations were substituted for the filtered concentrations in these samples, and those values are highlighted in the Supporting Information (Table S1). This was justified on the basis that contamination is more likely during filtration compared to loss of mass in acidified unfiltered samples. With the Ca^{2+} substitutions, 28 of the 33 samples showed charge balance errors within ±20% (corresponding to charge balances better than ±0.1 meq/L), which is considered a reasonable charge balance for snow samples (Clow et al., 2002). However, the remaining 5 samples had charge balance errors > −50% due to elevated Cl^- concentrations. Thus Cl^- concentrations from the corresponding duplicate snow pit sample were used for these 5 samples for charge balance calculations, as highlighted in the Supporting Information (Table S1). With the above corrections, all samples were charge balanced within ±20%.

For nearly all elements, concentrations measured on the field blank (for both unfiltered and filtered fractions) and laboratory blank were much lower than concentrations measured on snow samples (Supporting Information Table S1). However, Ag, Be, Cd, Mo, Se, and filtered Zn were disregarded from further analysis, and are not discussed further in this paper, because concentrations of Ag, Be, Cd, and Mo were similar (within a factor of two) in the blanks and samples, Se was below D.L. in the blanks and samples, and Zn showed substantial contamination in nearly all filtered samples (where filtered concentration ≫ unfiltered concentration). For some other elements in Dec–March (pre-dust) samples, unfiltered concentrations were substituted for filtered concentrations where the latter exceeded the former. This substitution involved 11 samples for Ba, 7 for Sr, 3 for Pb, and 2 for Ni out of 33 samples for each, as highlighted in the Supporting Information (Table S1). Again, this was justified on the basis that contamination is more likely during filtration compared to loss of mass in acidified unfiltered samples. For filtered samples, concentrations below the detection limit (Fe, Cu, and Tl in nearly all filtered samples, and Ba, K, Pb, and Sr in some filtered samples) were set as 1/2 the detection limit in order to calculate the particulate fraction of these elements.

2.5. Dust sample collection and analyses

In order to make a direct measurement of dust chemistry, samples of the 30 March, 5 April, and 11–12 April dust layers were collected by scraping a wide-mouth 250 mL FLPE bottle across the exposed dust layer along the snow pit wall. Samples of the 30 March dust layer were collected on 3 April at Upper and Lower Neffs, samples of the 30 March and 5 April dust layers were collected on 10 April at Upper and Lower Bells, and samples of all three dust layers were collected on 15 April and 17 April at Upper and Lower Cardiff and Desolation and Dog, respectively. Samples targeting each dust layer were melted and composited in three separate clean 1 L FLPE bottles. Dust was allowed to settle for ~20 h (based on settling velocity for silicate particles >1 μm) and melt water was carefully decanted. Dust and remaining overlying water was transferred to clean PPCO tubes, concentrated further by centrifugation (1000 RCF for 5 min), and melt water was successively decanted to isolate dust. As a final step, dust was allowed to dry in a laminar flow hood for several days.

Measuring the concentration of trace elements in dust poses the challenge of analyzing a leachate containing large concentrations of major components (e.g. Ca, Mg, Fe, Al) that can bias the accuracy of the result obtained for the trace elements. For these “matrix loaded” solutions, the more commonly used external calibration method lacks the accuracy needed for meaningful comparisons. The so-called standard addition method, in which increasing amounts of analyte are added to several aliquots of sample and then each of these mixtures are tested, provides more accurate results for trace element analysis when the sample matrix load is high (Rabb and Olesik, 2008). However, the best results are obtained when an isotope dilution (ID) method is available. ID-ICP-MS relies on the addition (spiking) of an enriched isotope of the element of interest followed by the measurement of the ratio between this isotope and a different one, normally the most abundant isotope free of interferences available. Because all isotopes from an element can be assumed to behave identically through the different processes affecting the transport and ionization at the mass-spectrometer introduction system, and because fractionation in the ICP interface can be corrected for by using isotopic standards, ID-ICP-MS is considered the best method for obtaining accurate concentrations in materials with complex matrices and therefore it is the method of choice for certifying reference materials (Beauchemin, 2006; Klingbeil et al., 2001).

Our method for analyzing the elemental concentrations in dust was a combination of standard addition and ID-ICP-MS. About 100 mg of dry dust from each dust layer was leached in ~5 g of cold 5% v/v HNO_3 prepared from concentrated nitric acid (Seastar) and Milli-Q water. After adding the acid to the weighted dust, the mixture was vortexed and left for one day at 22 °C, after which it was centrifuged and diluted by

weight using ~2 g of clear supernatant and 10 g of 5% v/v HNO_3. A ten-fold dilution from this solution was used to measure: 1) Al, K, Ca, and Fe using a standard addition method; and 2) Mg, Cu, Sr and Ba using ID-ICP-MS, by spiking with a calibrated mixed spike prepared from individual 10 μg/g solutions (Inorganic Ventures Inc.) of ^{25}Mg, ^{65}Cu, ^{86}Sr and ^{137}Ba. The remaining elements (Li, Be, Na, V, Cr, Mn, Co, Ni, As, Se, Cd, La, Ce, Nd, Pb, Th and U) were measured using a standard addition method on the first dilution. Consistency of this method has been extensively monitored using two reference soil materials (ZC73007 soil and CMI7004 loam), for which long-term reproducibility is better than 10% for most elements and as good as 2% (n = 32, over six months).

The cold leach with 5% v/v HNO_3 was not a total digestion of the dust, but an extraction process meant to dissolve the more accessible fraction consisting of cations adsorbed on clays and sesquioxides, and minerals with high reactivity in 5% v/v HNO_3, e.g. carbonates, Fe and Mn oxides, and some sulfates (Lawrence et al., 2010). Silicates were not dissolved by this method, and some minerals with very high solubility (such as halite) were likely lost by decanting melt water from dust sample bottles. Relative to weaker extraction methods (e.g. acetic acid and/or dilute HCl), HNO_3 (5% v/v) may potentially mobilize elements stabilized in organic matter via oxidation. However, because the goal was to compare dust chemistry to chemistry measured in snowpack, the dust was extracted in a similar manner as melted snow samples (5% and 2.4% v/v HNO_3, respectively). Comparisons to other studies that used complete digestion to analyze lake sediment (Reynolds et al., 2010) or upper continental crustal material (Wedepohl, 1995) must therefore be viewed as semi-quantitative comparisons only. However, our dust-leaching method is more directly comparable to the extractable + organic fraction measured by sequential extraction in Lawrence et al. (2010), who used 1 M NH_4Ac to leach the extractable fraction and 1 M (6.3% v/v) HNO_3 to leach the organic-associated fraction. They define this fraction as "available"; we use the same terminology to simplify comparisons with their results.

Mineralogy of dust layers was analyzed using QEMSCAN, an instrument that combines high-resolution electron microscopy (down to ~2 μm resolution) and rigorous statistical evaluation, allowing for quantification of mineral abundances. A field scan was performed on subsamples of dry dust from each dust layer mounted in 25 mm epoxy plugs.

2.6. Ancillary data

SWE, snowpack depth, air temperature, and soil moisture data for winter 2009–10 were obtained from three SNOTEL sites located within the central Wasatch sampling area: Snowbird (2938 m a.s.l.), Brighton (2667 m a.s.l.), and Mill-D North (2733 m a.s.l.) (Fig. 1) (SNOTEL, 2011). The average elevation of the SNOTEL sites (2780 ± 140 m a.s.l.) is similar to the average elevation of the 12 snow sampling locations (2690 ± 170 m a.s.l.), and SWE was similar between the SNOTEL sites and the sampling locations (Fig. 3). These similarities indicate that SNOTEL data are reasonably representative of the conditions found at the sampling sites.

3. Results

3.1. Trace and major element concentrations in snowpack

Whereas a large number of elements were analyzed in the snow samples, the main text of this paper focuses on concentrations and loads of 12 elements: 8 trace elements that are on the USEPA List of Hazardous Air Pollutants (As, Co, Cr, Hg, Mn, Ni, Pb, and Sb; USEPA, 1990), and 4 alkaline/alkaline earth elements that are typically found in the soluble fraction in snowpack (Ca, K, Na, and Sr; Grotti et al., 2011), which we refer to as "major" elements. Additional figures and tables showing data for other elements are provided in the Supporting Information.

The concentration of all measured trace elements and major ions increased during the period of sampling (Supporting Information Figs. S4 and S5). The change in concentration occurred abruptly, corresponding to the period between 27 March and 3 April when the first dust layer was deposited. Variation between duplicate snow samples (reflecting snowpack spatial heterogeneity, analytical errors, or sampling differences for snow column and bottle scrape samples) was much less than variation between concentrations measured in March and April samples (Supporting Information Figs. S4 and S5).

In response to the obvious differences between March and April snowpack chemistry, the data were divided into two groups, where "Dec–March" and "Dec–April" refer to total winter snow accumulation during December through March (i.e., samples collected on 18, 25, and 27 March 2010) and December through April (i.e., samples collected on 3, 10, and 15 April 2010), respectively (Table 1). Average trace and major element concentrations were elevated in Dec–April (n = 12) relative to Dec–March (n = 13) snowpack, as shown in Figs. 4 and 5, respectively. Other trace elements are shown in Supporting Information Fig. S6.

To determine whether differences in elemental concentrations measured in Dec–March samples (n = 13) and Dec–April samples (n = 12) were statistically significant, data from the two groups were compared using a paired Student's t-test with a two-tailed distribution and heteroscedastic variance. Only p-values <0.01 were considered significant. The bulk (unfiltered) concentration of all measured elements (Al, As, Ba, Ca, Co, Cr, Cu, Fe, Hg, K, Li, Mg, Mn, Na, Ni, Pb, Sr, Sb, Ti, Tl, U, V, and Zn) showed statistically significant increases in Dec–April relative to Dec–March snowpack (Figs. 4 and 5, Supporting Information Fig. S6). MeHg concentrations were low (<0.2 ng/L) in all samples. Although dust-containing samples were slightly elevated in MeHg, the limited number of samples (n = 10, of which only 3 samples were dust-free snowpack) did not allow for a robust comparison of the two groups.

3.2. Element partitioning between particulate and soluble fractions in snowpack

The fraction of trace and major elements associated with the >0.45 μm (calculated as the difference between unfiltered and filtered concentrations) and the <0.45 μm (filtered) fractions are hereby referred to as the "particulate" and "soluble" fractions, respectively. Although 0.45 μm is an arbitrary cutoff size between particulate and soluble fractions, as elements may be associated with fine particles <0.45 μm, we use it to provide information on the origin of the elements and to provide insight into their potential fate in the environment, as performed by Bacardit and Camarero (2010). Because particles were not digested prior to analysis (as described in Section 2.2), the actual trace and major element mass associated with the particulate fraction is likely underestimated; however, the elemental mass extracted from the particles by 2.4% v/v HNO_3 is a more reasonable representation of potential influences to snowmelt chemistry relative to mass extracted via complete digestion.

As was observed for the bulk chemistry, the particulate concentrations of all measured elements were significantly elevated in Dec–April relative to Dec–March snowpack (Figs. 4 and 5, Supporting Information Fig. S6). The soluble concentrations of the major elements (Ca, K, Mg, Na, Sr) showed significant increases between Dec–March and Dec–April, but only a subset of the trace elements (As, Al, Ba, Hg, Mn, U, and V) showed significantly higher soluble concentrations in Dec–April relative to Dec–March snowpack. The soluble concentrations of the remaining trace elements (Co, Cr, Cu, Fe, Ni, Pb, Sb, Ti, and Tl) were not significantly different between the two groups. Accordingly, the overall increase in concentrations between Dec–March and Dec–April snowpack was primarily in the particulate fraction

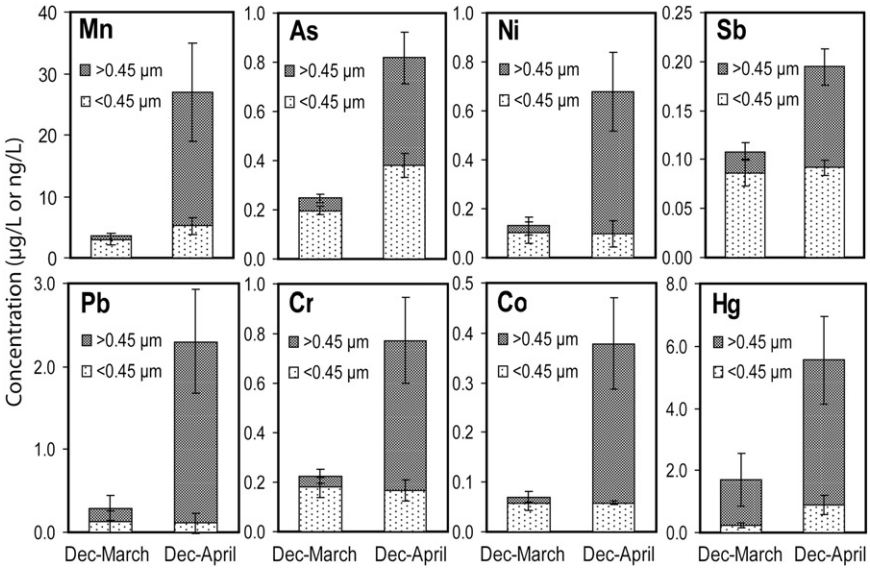

Fig. 4. Average trace element concentrations associated with the particulate (>0.45 μm) and soluble (<0.45 μm) fractions in December–March (n = 13) and December–April (n = 12) snowpack. Error bars represent ±1 s.d. Concentrations are μg/L for all elements except Hg, which is ng/L.

for the trace elements (Fig. 4 and Supporting Information Fig. S6), and in the soluble fraction for the major elements (Fig. 5).

For the major anions, ANC (i.e. HCO_3) was only measured on unfiltered samples, and Cl, NO_3, and SO_4 were only measured on filtered samples; thus partitioning between particulate and soluble fractions was not determined. However, the soluble concentrations of Cl, NO_3, and SO_4 were significantly elevated in Dec–April relative to Dec–March snowpack (Supporting Information Fig. S7). ANC was also significantly elevated in Dec–April snowpack. Likewise, pH was significantly higher in Dec–April (mean = 7.5 ± 0.7) relative to Dec–March (mean = 5.6 ± 0.7) melt water. The increase in ANC, although only measured on unfiltered samples, was likely due to soluble carbonate minerals which act to increase pH and buffering capacity (e.g. Rhoades et al., 2010).

3.3. March versus April snowpack

Re-sampling of the Dec–March strata of snowpack and exclusive sampling of the April strata at the Dog and Desolation sites indicates that the Dec–March snowpack was stable throughout the sampling period, with limited vertical mixing by melt water percolation, and that the majority of elemental loading occurred in April (Figs. 6 and 7, Supporting Information Figs. S8 and S9). Furthermore, because April snow pits at Dog and Desolation were excavated within 50 to 100 m of corresponding March snow pits, the re-sampling shows high spatial reproducibility of elemental concentrations in the Dec–March snowpack.

4. Discussion

4.1. Effect of dust on snowpack chemistry

The increase in trace and major element concentrations between Dec–March and Dec–April snowpack reflects temporal differences due to dust deposition, although the concern that it might reflect spatial differences between March and April sampling locations, or seasonal differences in precipitation chemistry (besides dust), should be addressed. April sites as a group are closer to the urban area (Fig. 1), indicating the possibility that elevated concentrations are related to urban influences. However, paired Student's t-tests comparing groups of sites separated by linear distance to the urban area (i.e. Group 1 (close to urban area): Lower Neffs, Upper Neffs, Lower Bells, Upper Bells, Lower White Pine, Upper White Pine; and Group 2 (distal to urban area): Lower Cardiff, Upper Cardiff, Dog, Desolation, Lower Guardsman, Upper Guardsman) showed no significant difference for any of the measured elements. Furthermore, re-sampling of Dog and Desolation sites (distal to urban area; Fig. 1) in April showed that the April strata of the snowpack contained elevated elemental concentrations relative to the Dec–March strata of the snowpack for all trace and major elements (Figs. 6 and 7, Supporting Information Figs. S8 and S9), demonstrating that elevated concentrations are associated with April deposition rather than proximity to the urban area.

With respect to potential seasonal differences in precipitation chemistry between March and April, increased SWE during April (Fig. 3) reflects continued snow accumulation which potentially

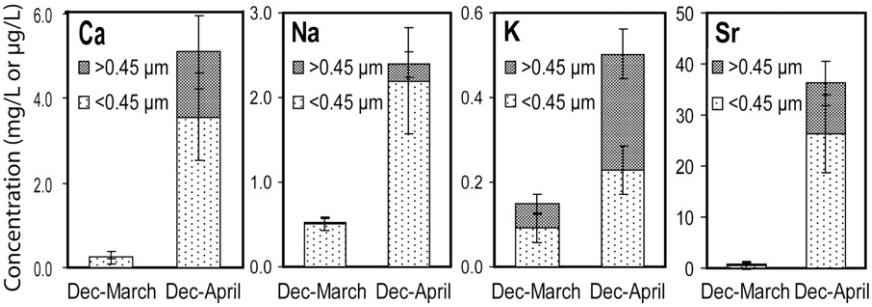

Fig. 5. Average major element concentrations associated with the particulate (>0.45 μm) and soluble (<0.45 μm) fractions in December–March (n = 13) and December–April (n = 12) snowpack. Error bars represent ±1 s.d. Concentrations are mg/L for all elements except Sr, which is μg/L.

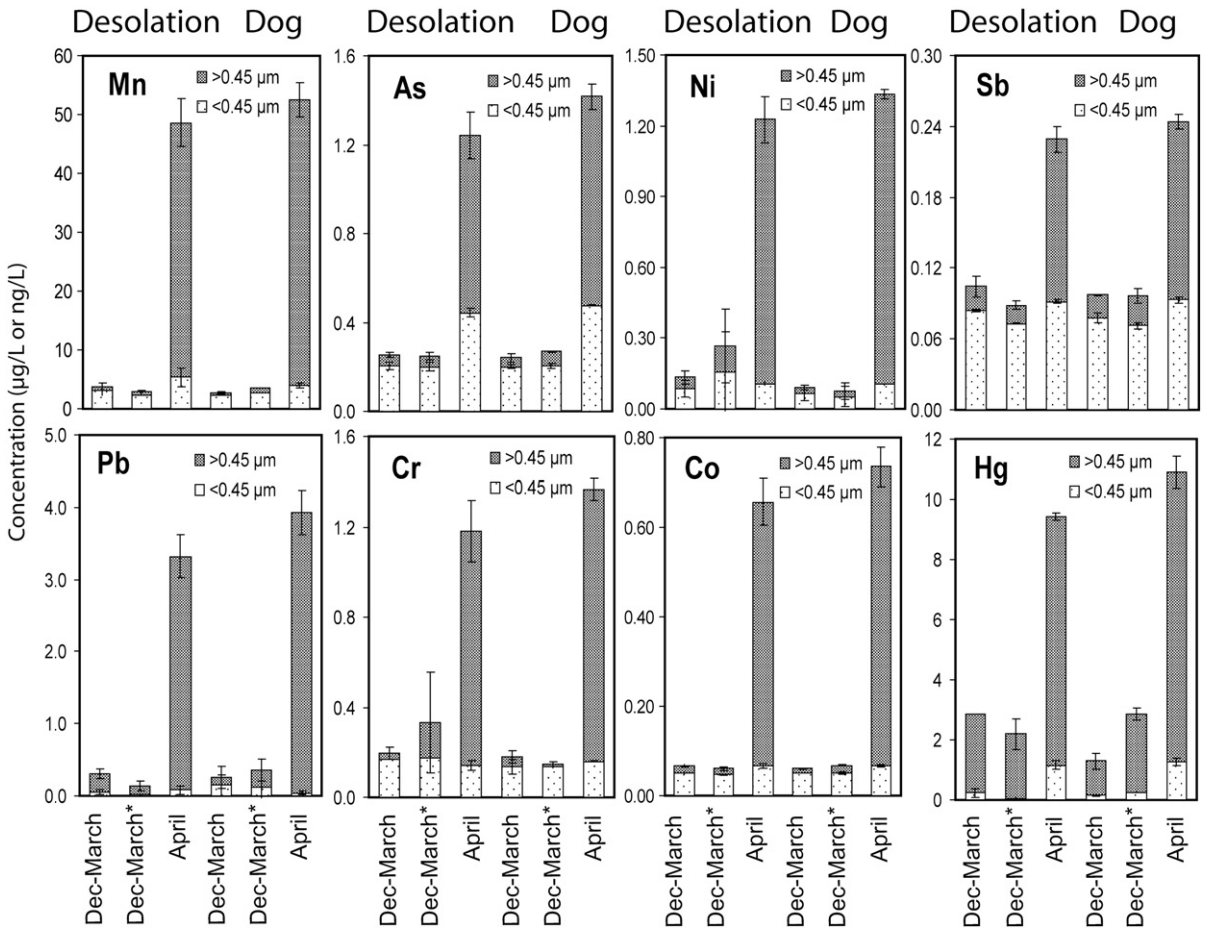

Fig. 6. Trace element concentrations associated with the particulate (>0.45 μm) and soluble (<0.45 μm) fractions at Desolation and Dog sampling sites. December–March snowpack was sampled during March ("Dec–March") and re-sampled at a nearby (<100 m) location during April ("Dec–March*"). April snowpack was sampled exclusively in order to compare element concentrations in December–March versus April snowpack. Values are average concentrations of duplicate snow columns collected from each snow pit, and error bars represent ±1 s.d. Concentrations are μg/L for all elements except Hg, which is ng/L.

contained elevated concentrations of trace and major elements. For example, Kuhn et al. (1998) observed that major ion concentrations in the Tyrolean Alps, which were relatively low in winter snowpack (including March), increased sharply during April due to increased temperature gradients and associated strong atmospheric mixing and local convection. However, while elemental deposition to April snowpack may be enhanced by warmer spring conditions, the abrupt change in trace and major element concentrations between samples

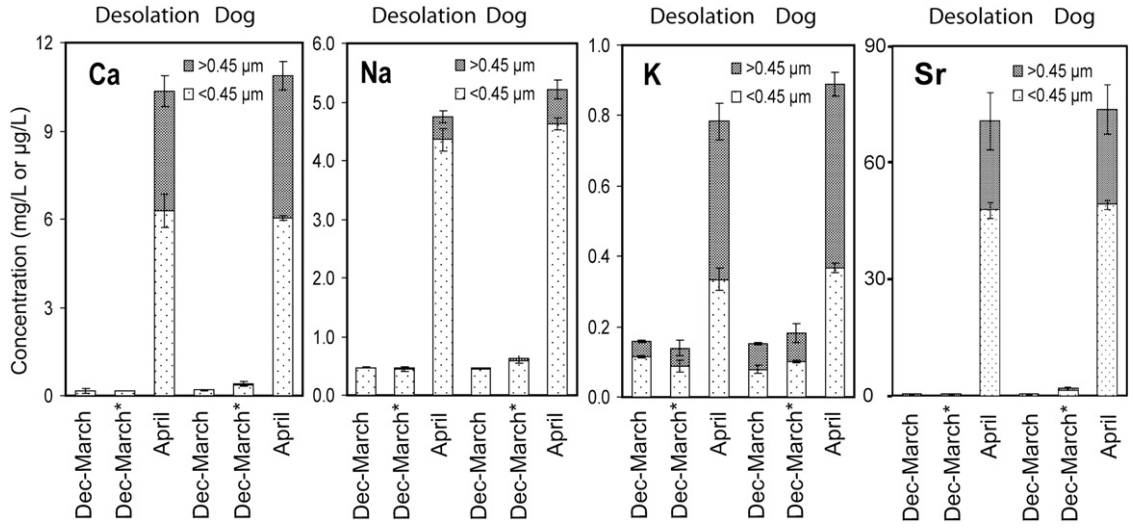

Fig. 7. Major element concentrations associated with the particulate (>0.45 μm) and soluble (<0.45 μm) fractions at Desolation and Dog sampling sites. December–March snowpack was sampled during March ("Dec–March") and re-sampled at a nearby (<100 m) location during April ("Dec–March*"). April snowpack was sampled exclusively in order to compare element concentrations in December–March versus April snowpack. Values are average concentration of duplicate snow columns collected from each snow pit, and error bars represent ±1 s.d. Concentrations are mg/L for all elements except Sr, which is μg/L.

collected 27 March and 3 April (Supporting Information Figs. S4 and S5) indicates that the difference was not consistent with a gradual shift in elemental concentrations that would be expected from seasonal effects.

The most obvious difference between Dec–March and April snow accumulation is the deposition of dust beginning 30 March. Three distinct dust layers were observed in the April snowpack (deposited 30 March, 5 April, and 11–12 April; Fig. 2). Dust layers were not observed in the Dec–March snowpack. The delivery of trace elements via dust is indicated by their association with the particulate (>0.45 μm) size fraction (Fig. 4), and by direct measurement of these elements in leached dust samples (Supporting Information Table S4).

Of the trace and major elements which showed significant increases in the soluble fraction between Dec–March and Dec–April snowpack, the majority (including Ba, Ca, Cl, K, Li, Mg, Na, SO_4, and Sr; Fig. 5, Supporting Information Figs. S6 and S7) are associated with evaporite minerals common in Great Basin playas, such as halite, gypsum, calcite, and dolomite (e.g. Reheis et al., 2002). Dry lakebeds are a significant source of salt aerosols, which may be transported as particles >0.45 μm (Abuduwailli et al., 2008). Regardless of particle size, the prevalence of these elements in the soluble fraction may reflect the dissolution of these relatively high solubility minerals during melting of the snow samples prior to subsampling, further yielding the relatively high pH of the samples collected during April.

4.2. Dust composition and possible source(s)

Determining dust provenance or matching the chemistry of the dust in the snowpack to dust from the emission source(s) were not primary goals of this study; however, measurement of dust chemistry provides direct evidence of the effect of dust on snowpack chemistry, and potentially allows for a comparison of chemistry between different dust events. The dust layers deposited 30 March, 5 April, and 11–12 April 2010 show differences in elemental composition (Supporting Information Table S4), possibly reflecting different dust emission sources. However, QEMSCAN results show that all of the dust layers have similar mineralogy, with average aerial abundances of 24.5 ± 1.1% plagioclase, 20.8 ± 0.7% quartz, 15.3 ± 1.3% micas, 14.3 ± 4.4% feldspar, 10.5 ± 3.6% amphibole, 5.3 ± 1.9% calcite, 2.6 ± 0.8 chlorite, and 2.4 ± 0.4% dolomite (Supporting Information Table S5).

Although locating the specific source of dust emissions to the central Wasatch snowpack is beyond the scope of this paper, HYSPLIT 24 h back trajectories (Draxler and Rolph, 2003) indicate that air masses associated with dust storms on 30 March, 5 April, and 11–12 April originated in southwestern Utah (Supporting Information Fig. S10). Dust events in the Great Basin are common during late winter to early spring in association with cyclonal cold fronts (Steenburgh et al., in press), when elevated wind speeds are most frequently observed (Jewell and Nicoll, 2011), coinciding to the time period of maximum snowpack accumulation. Substantial snow deposition typically arrives with the cold fronts.

4.3. Enrichment factors in snowpack and dust

In order to evaluate the relative contribution from natural (i.e. continental crust) versus anthropogenic sources, the concentrations of trace and major elements in snow and dust aerosol samples are commonly expressed in the form of crustal enrichment factor (EF_{ucc}) (Bacardit and Camarero, 2010; Grotti et al., 2011; Reheis et al., 2009; Veysseyre et al., 2001; Zoller et al., 1974). EF_{ucc} is defined as the concentration ratio of a given element to that of Al (or any other element that is representative of crustal material) normalized to the same reference concentration ratio characteristic of the upper continental crust (UCC) given by Wedepohl (1995): $EF_{ucc} = ([X]_s/[Al]_s)/([X]_{ucc}/[Al]_{ucc})$, where X is the element of interest and the subscript s denotes concentration in the sample. Enrichment factors between 0.1 and 10 indicate that the element of interest is likely derived from crustal sources, whereas enrichment factors >10 indicate inputs from other sources. Values from 10 to 500 are moderately enriched, whereas values over 500 are strongly enriched and indicate an anthropogenic contribution. EF_{ucc} was calculated for snowpack samples (using unfiltered concentrations) and dust layer samples. Enrichment factors should be interpreted with caution because of the variable concentration of the crust and because our snow and dust samples were not completely digested and thus total concentrations were not measured (Grotti et al., 2011). Thus EF_{ucc} calculated in this study may not be directly comparable to those calculated elsewhere, but because our snow and dust samples were prepared and analyzed by practically equivalent methods the samples can be compared to one another. EF_{ucc} values calculated here for snow samples are, however, directly comparable with those found in Veysseyre et al. (2001).

The enrichment factors for Dec–March snowpack (n = 13), Dec–April snowpack (n = 12), and dust layer samples (n = 3) are shown in Fig. 8. When $0.1 < EF_{ucc} < 10$ the corresponding element is likely crustally derived; i.e., Ba, Fe, Sr, V, K, Co, Mn, Ni, and Cr. In contrast, other elements are enriched relative to UCC; i.e., Cu, Pb, Hg, Zn, As, and Sb. Notably, for Zn, As, and Sb the enrichment is much greater in the Dec–

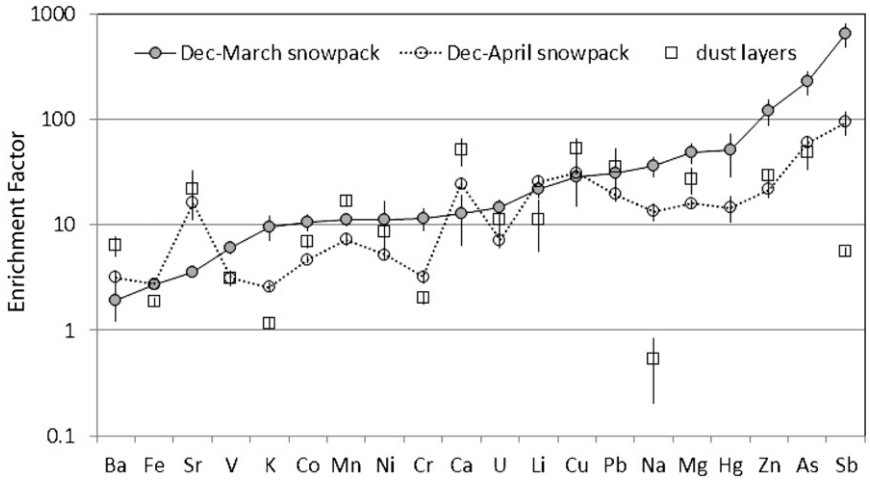

Fig. 8. Crustal enrichment factor (EF_{ucc}) for December–March snowpack (pre-dust; n = 13), December–April snowpack (including dust, n = 12), and dust layers (n = 3). Values shown in the plot are averages and error bars represent ±1 s.d. For convenience, values are ranked in order of ascending EF_{ucc} for December–March snowpack. Hg concentrations were not measured on dust samples.

March snowpack relative to the Dec–April snowpack or dust layers, possibly reflecting the influence of local anthropogenic inputs to the winter snowpack, e.g. winter inversions. Indeed, Sb was strongly enriched in snowpack samples, but was near crustal values in the dust samples, reflecting lack of Sb sources in the dust.

The enrichment signatures show that Dec–April snowpack is strongly influenced by dust deposition (Fig. 8). The EF_{ucc} signature of Dec–April snowpack tracks closely the EF_{ucc} signature of dust, both even crossing that of the Dec–March snowpack. This demonstrates that dust imparts the elemental signature to the Dec–April snowpack.

The EF_{ucc} for Sr and Ca is elevated in both the dust and Dec–April snowpack, reflecting the influence of carbonates that are common in Great Basin playas. On the basis of QEMSCAN measurements, calcite and dolomite together comprise nearly 8% of the dust (by area; Supporting Information Table S5), but this value, although substantial, is likely underestimated because micro-crystalline calcite is not measured by QEMSCAN. The EF_{ucc} for Na is elevated in Dec–March snowpack, consistent with the known elevated salinity in Wasatch winter snowpack, which may reflect northerly storm tracks across Great Salt Lake or widespread use of road salt in the Salt Lake Valley (Arens, 2010; Cerling and Alexander, 1987). In contrast, the EF_{ucc} for Na in dust is near unity, possibly reflecting the lack of influence of Great Salt Lake, since the dust is transported from the south to the Wasatch Front by southerly pre-storm winds, or it may reflect loss of the most soluble minerals (e.g. halite) during the dust isolation procedure. That the EF_{ucc} for Na in Dec–April snowpack is likewise similar to crustal values (EF_{ucc} of ~10) suggests lack of halite enrichment in the dust, in contrast to enrichment in other playa-associated minerals (e.g. carbonates).

Enrichment in anthropogenic elements in dust relative to UCC, although smaller in magnitude than the enrichment found in dust-free Dec–March snowpack, is consistent with observations by Castillo et al. (2008), Lawrence and Neff (2009), and Lawrence et al. (2010). It is likely that the enrichment in trace elements in the dust samples relative to UCC is at least partially explained by entrainment of these pollutants as the air masses (and dust) traverse the industrialized basins on the west flank of the Wasatch Mountains.

Enrichment in anthropogenic elements in dust is also consistent with the results from Reynolds et al. (2010), who found that lakebed sediment from the past 140 years at two lakes in the Uinta Mountains of Utah (~100 km east of the Wasatch) was elevated in elements associated with ore deposits (e.g. As, Cd, Cu, Mo, Pb, Sb, and Sn) due to exogenous dust. They determined that the source of the heavy metal-laden dust was likely mining and smelting activities along the Wasatch Front.

As was observed by enrichment factors relative to UCC, Wasatch dust is generally enriched in elements associated with playa minerals or anthropogenic activities relative to San Juan dust (Lawrence et al., 2010). Elemental concentrations measured in Wasatch dust relative to those reported for San Juan dust (f), where the latter was measured by similar extraction methods to our study (Lawrence et al., 2010), shows that Wasatch dust is moderately enriched in K, Li, Pb, Sr, and Y ($1.2<f<2.0$) and greatly enriched in Mg, Ca, Co, and Cr ($f>2.0$) (Supporting Information Table S6). Wasatch dust is also enriched in As ($f=3.3$), which is associated with both evaporite basins in central Utah (Ryker, 2001) and anthropogenic activities. In contrast, Wasatch dust is similar to San Juan dust in concentrations of Fe, Cd, Ce, Mo, Ni, V, and Zn ($0.8<f<1.2$), and depleted in Al, Na, Ba, Cu, Be, and La ($f<0.8$). The relative depletion of the playa-associated Na was also observed for comparisons to UCC, possibly reflecting relative lack of halite in the dust (as described above). The relative depletion of anthropogenic-associated Cu may reflect additional sources in the San Juan Mountains. The variability in dust chemistry between the Wasatch and San Juan Mountains likely reflects different source areas of dust and differences in air mass trajectories.

4.4. Comparison of Wasatch snowpack chemistry to other locations

Average bulk (unfiltered) concentrations of trace elements in Wasatch snowpack (with and without dust) were compared to measurements made in the Central Pyrenees (Bacardit and Camarero, 2010), the Dolomites (Gabrielli et al., 2008), and Mt. Everest (Kang et al., 2007). Wasatch samples containing dust (Dec–April snowpack) were elevated by a factor of two or more for most trace elements relative to the other locations, with the exception of Sb, which was elevated at Mt. Everest (Table 2). Pre-dust Wasatch samples (Dec–March snowpack) were elevated only in Fe and Al, with similar concentrations (±1 s.d.) of As, Ba, Cr, Co, Cu, Mn, Ni, Pb, U, V, and Zn relative to the snowpack from locations (Table 2). This excludes Sb and Pb, which were higher and lower, respectively, at Mt. Everest. It also

Table 2
Comparisons of trace element concentrations in Wasatch snowpack (pre- and post-dust) and snowpack from other locations. All results reported here are for bulk (unfiltered) samples. Units are μg/L for everything except Hg, which is ng/L.

	Wasatch (pre-dust)	Wasatch (including dust)	Central Pyrenees (Spain)	Dolomites (Italy)	Mt. Everest
n	13	12	44	366	14
Al	44.4 ± 12.4	538 ± 121	8.61 ± 9.31		4.5 ± 4.1
As	0.25 ± 0.02	0.82 ± 0.14			0.18 ± 0.30
Ba	0.69 ± 0.44	14.6 ± 3.45		1.3 ± 2.7	
Co	0.07 ± 0.01	0.38 ± 0.09		0.05 ± 0.08	
Cr	0.22 ± 0.06	0.77 ± 0.18		0.10 ± 0.21	0.03 ± 0.07
Cu	0.23 ± 0.12	3.00 ± 0.66	0.06 ± 0.07	0.72 ± 1.86	0.34 ± 0.37
Fe	48.9 ± 17.0	593 ± 166	9.01 ± 9.77	27.3 ± 74.6	11.5 ± 4.3
Hg	1.70 ± 0.85	5.55 ± 1.53			
Mn	3.33 ± 0.73	26.9 ± 8.0	0.50 ± 0.37	4.3 ± 14	2.00 ± 2.10
Ni	0.12 ± 0.05	0.68 ± 0.19	0.06 ± 0.18		
Pb	0.29 ± 0.07	2.30 ± 0.62	1.92 ± 3.22	1.8 ± 2.9	0.01 ± 0.01
Sb	0.11 ± 0.01	0.19 ± 0.02		0.08 ± 0.36	2.95 ± 2.82
Ti	3.37 ± 1.21	25.3 ± 6.5	0.46 ± 0.58	2.8 ± 6.9	
U	0.02 ± 0.00	0.12 ± 0.03		0.009 ± 0.023	
V	0.18 ± 0.03	1.16 ± 0.29		0.22 ± 0.37	0.14 ± 0.07
Zn	3.49 ± 1.00	7.66 ± 1.18	2.72 ± 3.23	3.5 ± 6.2	2.03 ± 2.4
Source	This study	This study	Bacardit and Camarero (2010)	Gabrielli et al. (2008)	Kang et al. (2007)
Sampling period	Dec 2009–March 2010	Dec 2009–April 2010	Dec 2004–March 2005	Dec 1997–April 1998	May 2005
Sample type	Snow pit	Snow pit	Snow pit	Fresh snow	Fresh snow
Sampling strategy	Regional samples	Regional samples	Altitude gradient	Weekly collection; regional	Altitude gradient
Extraction method	2.4% HNO_3 solution	2.4% HNO_3 solution	Sum of dissolved and particulate (1% HNO_3 on filtrate; filters digested to measure particulate fraction)	2% HNO_3 solution	1% HNO_3 solution

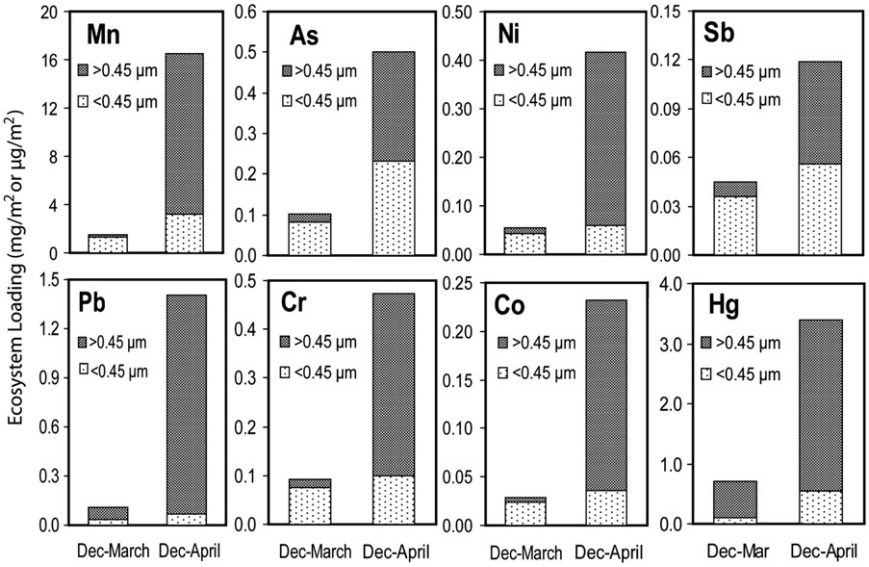

Fig. 9. Average trace element ecosystem loading associated with the particulate (>0.45 μm) and soluble (<0.45 μm) fractions in December–March and December–April snowpack. Concentrations are mg/m^2 for all elements except Hg, which is μg/m^2.

excludes Ti, which was lower in the Central Pyrenees. These results indicate that ambient (pre-dust) Wasatch snowpack chemistry does not contain elevated concentrations of anthropogenic (and other) trace elements relative to limited data from other mid-latitude mountain snowpack; whereas dust contributes relatively greater amounts of trace elements to Wasatch snowpack.

The soluble fraction of major ions from the Wasatch (pre-dust) was compared to results from other studies where snow was collected from snow pits at or near maximum accumulation including the Wasatch (Arens, 2010), Rocky Mountains (Clow et al., 2002; Turk et al., 2001), San Juan Mountains (Lawrence et al., 2010), Cascade–Sierra Nevada Mountains (Laird et al., 1986), and Austrian Alps (Winiwarter et al., 1998) (Supporting Information Table S7). Wasatch snowpack (pre-dust) is elevated by a factor of 2 or more in Mg, Na, and Cl relative to the other locations with average concentrations of 27 ± 2, 22 ± 3, and 28 ± 17 μeq/L, respectively. Arens (2010) likewise reported elevated concentrations of these ions, although that study did not mention absence/presence of dust layers. Ca, K, and SO_4 were similar in concentration to other locations (± 1 s.d.), in contrast to the results of Arens (2010) who found elevated concentrations of these ions in Wasatch snowpack. NO_3 was depleted in Wasatch snowpack (1.9 ± 0.3 μeq/L) relative to previously reported values from the Wasatch, Rocky Mountains, San Juan Mountains, and Austrian Alps (>7 μeq/L), but similar to concentrations reported for the Cascade–Sierra Nevada Mountains. These results indicate that ambient (pre-dust) Wasatch snowpack contains elevated concentrations of salts (Mg, Na, and Cl) compared to other locations, including the Pacific Ocean-influenced Cascade–Sierra Nevada Mountains, possibly due to downwind relationship to the saline playas surrounding nearby Great Salt Lake (Arens, 2010). The relative depletion in NO_3 is surprising since the urban Wasatch Front is a potential NO_3 source, but may reflect a relative lack of agriculture or other sources in the Great Basin desert.

The soluble fraction of post-dust Wasatch snowpack was compared to other studies which specifically sampled dust layers contained in Rocky Mountain (Rhoades et al., 2010) and San Juan Mountain (Lawrence et al., 2010) snowpack (Supporting Information Table S8). Concentrations of Ca, Mg, Na, Cl, and SO_4 were at least a factor of two greater in the Wasatch snow (with dust) than concentrations reported in snow containing dust layers at other locations. In contrast, ANC (i.e. HCO_3) concentrations were a factor of two less than concentrations in Rocky Mountain snow containing dust. K concentrations were similar between the Wasatch and San Juan Mountains; both were a factor of ten greater than concentrations reported for the Rocky Mountain dust-containing snow. NO_3 in the Wasatch was a factor of two greater than the Rocky Mountain dust layer, but a factor of five less than the concentration in San Juan snowpack. These results indicate that Wasatch snowpack major ion chemistry is more heavily influenced by dust (for most ions) relative to Rocky Mountain snowpack (including the San Juan Mountains).

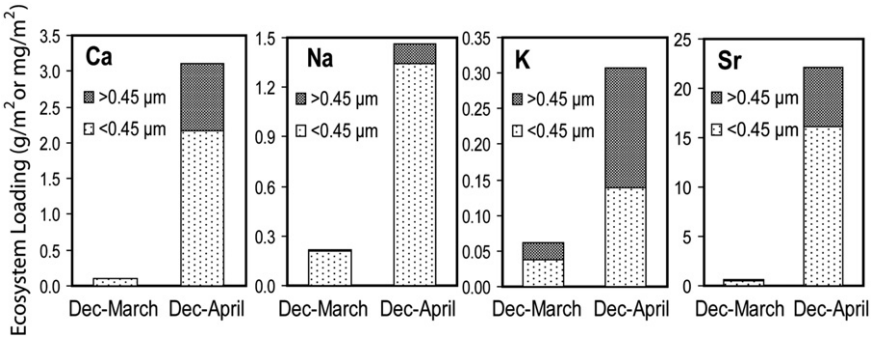

Fig. 10. Average major element ecosystem loading associated with the particulate (>0.45 μm) and soluble (<0.45 μm) fractions in December–March and December–April snowpack. Concentrations are g/m^2 for all elements except Sr, which is mg/m^2.

4.5. Ecosystem loading of trace and major elements

Ecosystem loading (μg, mg, or g/m^2) at each sampling site was calculated using measured elemental concentrations (ng, μg, or mg/L) and SWE (cm). Loads were averaged for the sites sampled in March and April, respectively. Since the entire snowpack was not sampled, the calculated loads do not include snow that fell prior to mid-December. Thus, loads were estimated only for Dec–March and Dec–April snowpack, respectively.

The majority of trace and major element loading occurred during April as a result of dust deposition (Figs. 9 and 10, Supporting Information Figs. S11 and S12). Given that dust loading to the central Wasatch during Spring 2010 was on the order of 10s of g/m^2 (A. Bryant, personal communication), and annual dust loading in the southwest United States is as high as 50 g/m^2 (Lawrence and Neff, 2009), calculated values of trace element loading on the order of 0.2 to 1.5 mg/m^2 for Co, Cr, Ni, and Pb (Fig. 9), major element loading on the order of 1.5 and 3 g/m^2 for Na and Ca, respectively (Fig. 10), are reasonable estimates. These loads are similar in magnitude to those presented for annual dust loads in Lawrence and Neff (2009). Although the majority of elemental loading is associated with April dust, a fraction of the loading is also due to pre-dust (ambient) snow deposition during Dec–March (Figs. 9 and 10, Supporting Information Figs. S11 and S12).

The soluble fraction of a given element may be a factor in determining its fate during spring snow melt, as soluble elements may be more likely flushed downstream and may be more prone to uptake by biota, while particulate elements may be retained in soil (Bacardit and Camarero, 2010). As, Sb, and the major elements were substantially loaded in the soluble fraction, whereas the remaining trace elements were primarily loaded in the particulate fraction (Figs. 9 and 10, Supporting Information Figs. S11 and S12). Further work is needed to understand the fate of these elements during snow melt.

5. Conclusions

Pre-dust trace element concentrations in Wasatch snowpack were surprisingly not elevated relative to limited data available from other mid-latitude mountain snowpack. Pre-dust Wasatch snowpack was, however, elevated in major ions Mg, Na, and Cl, possibly reflecting the influence of upwind Great Salt Lake playas or extensive use of road salts in the Salt Lake Valley. Enrichment relative to continental crust was observed in pre-dust snowpack for Zn, As, and Sb, likely reflecting urban and industrial input of these elements.

Dust storms, which frequently affect the Wasatch snowpack during spring months, significantly alter the chemistry of Wasatch snowpack. Post-dust Wasatch snowpack contained elevated concentrations of all trace and major elements relative to both pre-dust snowpack and snowpack from other locations. Although dust input increased element concentrations, it decreased crustal enrichment for Zn, As, and Sb, reflecting the playa-associated mineralogy of the dust. Of the dust-derived elements loaded to snowpack, some were immediately soluble (Na, Ca, K, Sr), and thus are expected to directly influence runoff chemistry, whereas others remained in the particulate phase (e.g. Cr, Hg, Mn, Pb) and have uncertain fate, and therefore influence, on runoff chemistry.

Acknowledgments

We wish to thank Maura Hahnenberger (U. of Utah) and Joel Karmazyn (Utah Dept. of Air Quality) for performing HYSPLIT modeling, Bonnie Baxter and Jaimi Butler (Great Salt Lake Institute) for providing technicians to help with field and laboratory work, in particular Kaitlyn Porter, and David Tingey (Brigham Young University) for generously providing equipment and time for ion chromatography and ANC measurements. We are grateful for the three anonymous reviewers whose comments greatly improved this paper and gave it more focused direction. Funding for the project was provided by an EPA RARE Region 8 grant. G.T.C. was funded by National Science Foundation GK-12 grant number DGE08-41233.

Appendix A. Supplementary data

Supplementary data to this article can be found online at http://dx.doi.org/10.1016/j.scitotenv.2012.05.077.

References

Abuduwailli J, Gabchenko MV, Xu JR. Eolian transport of salts — a case study in the area of Lake Ebinur (Xinjiang, Northwest China). J Arid Environ 2008;72:1843–52.
Arens SJT, 2010. Ion deposition in Wasatch Mountain snow: influence of Great Salt Lake and Salt Lake City. M.S. Thesis, University of Utah, 54 pp.
Ayling BF, McGowan HA. Niveo-eolian sediment deposits in coastal South Victoria Land, Antarctica: indicators of regional variability in weather and climate. Arct Antarct Alp Res 2006;38:313–24.
Bacardit M, Camarero L. Atmospherically deposited major and trace elements in the winter snowpack along a gradient of altitude in the Central Pyrenees: the seasonal record of long-range fluxes over SW Europe. Atmos Environ 2010;44:582–95.
Beauchemin D. Inductively coupled plasma mass spectrometry. Anal Chem 2006;78:4111–35.
Castillo S, Moreno T, Querol X, Alastuey A, Cuevas E, Herrmann L, et al. Trace element variation in size-fractionated African desert dusts. J Arid Environ 2008;72:1034–45.
Cerling TE, Alexander AJ. Chemical composition of hoarfrost, rime and snow during a winter inversion in Utah, USA. Water Air Soil Pollut 1987;35:373–80.
Clow DW, Ingersoll GP, Mast MA, Turk JT, Campbell DH. Comparison of snowpack and winter wet-deposition chemistry in the Rocky Mountains, USA: implications for winter dry deposition. Atmos Environ 2002;36:2337–48.
Correia A, Freydier R, Delmas RJ, Simoes JC, Taupin JD, Dupre B, et al. Trace elements in South America aerosol during 20th century inferred from a Nevado Illimani ice core, Eastern Bolivian Andes (6350 m asl). Atmos Chem Phys 2003;3:1337–52.
Draxler RR, Rolph GD. HYSPLIT (HYbrid Single-Particle Lagrangian Integrated Trajectory) model access via NOAA ARL READY. Silver Spring, MD: NOAA Air Resources Laboratory; 2003. Website (http://ready.arl.noaa.gov/HYSPLIT.php).
Ferrari CP, Clotteau T, Thompson LG, Barbante C, Cozzi G, Cescon P, et al. Heavy metals in ancient tropical ice: initial results. Atmos Environ 2001;35:5809–15.
Fortner SK, Lyons WB, Fountain AG, Welch KA, Kehrwald NM. Trace element and major ion concentrations and dynamics in glacier snow and melt: Eliot Glacier, Oregon Cascades. Hydrol Process 2009;23:2987–96.
Gabrieli J, Carturan L, Gabrielli P, Kehrwald N, Turetta C, Cozzi G, et al. Impact of Po Valley emissions on the highest glacier of the Eastern European Alps. Atmos Chem Phys 2011;11:8087–102.
Gabrielli P, Cozzi G, Torcini S, Cescon P, Barbante C. Trace elements in winter snow of the dolomites (Italy): a statistical study of natural and anthropogenic contributions. Chemosphere 2008;72:1504–9.
Gaspari V, Barbante C, Cozzi G, Cescon P, Boutron CF, Gabrielli P, et al. Atmospheric iron fluxes over the last deglaciation: climatic implications. Geophys Res Lett 2006;33:L03704.
Goldstein HL, Reynolds RL, Reheis MC, Yount JC, Neff JC. Compositional trends in aeolian dust along a transect across the southwestern United States. J Geophys Res 2008;113:F02S02.
Grotti M, Soggia F, Ardini F, Magi E. Major and trace element partitioning between dissolved and particulate phases in Antarctic surface snow. J Environ Monit 2011;13:2511–20.
Hong S, Barbante C, Boutron C, Gabrielli P, Gaspari V, Cescon P, et al. Atmospheric heavy metals in tropical South America during the past 22 000 years recorded in a high altitude ice core from Sajama, Bolivia. J Environ Monit 2004a;6:322–6.
Hong S, Boutron CF, Gabrielli P, Barbante C, Ferrari CP, Petit JR, et al. Past natural changes in Cu, Zn and Cd in Vostok Antarctic ice dated back to the penultimate interglacial period. Geophys Res Lett 2004b;31:L20111.
Hong S, Boutron CF, Barbante C, Hur SD, Lee K, Gabrielli P, et al. Glacial–interglacial changes in the occurrence of Pb, Cd, Cu and Zn in Vostok Antarctic ice from 240 000 to 410 000 years BP. J Environ Monit 2005;7:1326–31.
Hong S, Lee K, Hou S, Soon DH, Ren J, Burn LJ, et al. An 800-year record of atmospheric As, Mo, Sn, and Sb in central Asia in high-altitude ice cores from Mt. Qomolangma (Everest), Himalayas. Environ Sci Technol 2009;43:8060–5.
Jewell PW, Nicoll K. Wind regimes and aeolian transport in the Great Basin, U.S.A. Geomorphology 2011;129:1-13.
Kang SC, Zhang QG, Kaspari S, Qin DH, Cong ZY, Ren JW, et al. Spatial and seasonal variations of elemental composition in Mt. Everest (Qomolangma) snow/firn. Atmos Environ 2007;41:7208–18.
Klingbeil P, Vogl J, Pritzkow W, Riebe G, Muller J. Comparative studies on the certification of reference materials by ICPMS and TIMS using isotope dilution procedures. Anal Chem 2001;73:1881–8.
Kuhn M, Haslhofer J, Nickus U, Schellander H. Seasonal development of ion concentration in a high alpine snow pack. Atmos Environ 1998;32:4041–51.
Laird LB, Taylor HE, Kennedy VC. Snow chemistry of the Cascade–Sierra Nevada Mountains USA. Environ Sci Technol 1986;20:275–90.
Lawrence CR, Neff JC. The contemporary physical and chemical flux of aeolian dust: a synthesis of direct measurements of dust deposition. Chem Geol 2009;267:46–63.

Lawrence CR, Painter TH, Landry CC, Neff JC. Contemporary geochemical composition and flux of aeolian dust to the San Juan Mountains, Colorado, United States. J Geophys Res 2010;115:G03007.
Lee K, Hur SD, Hou S, Hong S, Qin X, Ren J, et al. Atmospheric pollution for trace elements in the remote high-altitude atmosphere in central Asia as recorded in snow from Mt. Qomolangma (Everest) of the Himalayas. Sci Total Environ 2008;404:171–81.
Marteel A, Gaspari V, Boutron CF, Barbante C, Gabrielli P, Cescon P, et al. Climate-related variations in crustal trace elements in Dome C (East Antarctica) ice during the past 672 kyr. Clim Chang 2009;92:191–211.
Mayo AL, Klauk RH. Contributions to the solute and isotopic groundwater geochemistry, Antelope Island, Great Salt Lake, Utah. J Hydrol 1991;127:307–35.
Munson SM, Belnap J, Okin GS. Responses of wind erosion to climate-induced vegetation changes on the Colorado Plateau. Proc Natl Acad Sci USA 2011;108: 3854–9.
Neff JC, Ballantyne AP, Farmer GL, Mahowald NM, Conroy JL, Landry CC, et al. Increasing eolian dust deposition in the western United States linked to human activity. Nat Geosci 2008;1:189–95.
Painter TH, Barrett AP, Landry CC, Neff JC, Cassidy MP, Lawrence CR, et al. Impact of disturbed desert soils on duration of mountain snow cover. Geophys Res Lett 2007;34:L12502.
Painter TH, Deems JS, Belnap J, Hamlet AF, Landry CC, Udall B. Response of Colorado River runoff to dust radiative forcing in snow. Proc Natl Acad Sci USA 2010;107: 17125–30.
Price D. Ground water in Utah's densely populated Wasatch Front area — the challenge and the choices. US Geological Survey water supply paper 2232; 1985. 71 pp.
Rabb SA, Olesik JW. Assessment of high precision, high accuracy inductively coupled plasma-optical emission spectroscopy to obtain concentration uncertainties less than 0.2% with variable matrix concentrations. Spectrochim Acta B 2008;63:244–56.
Reheis MC, Budahn JR, Lamothe PJ. Geochemical evidence for diversity of dust sources in the southwestern United States. Geochim Cosmochim Acta 2002;66: 1569–87.
Reheis MC, Budahn JR, Lamothe PJ, Reynolds RL. Compositions of modern dust and surface sediments in the Desert Southwest, United States. J Geophys Res 2009;114: F01028.
Reynolds RL, Mordecai JS, Rosenbaum JG, Ketterer ME, Walsh MK, Moser KA. Compositional changes in sediments of subalpine lakes, Uinta Mountains (Utah): evidence for the effects of human activity on atmospheric dust inputs. J Paleolimnol 2010;44:161–75.
Rhoades C, Elder K, Greene E. The influence of an extensive dust event on snow chemistry in the southern Rocky Mountains. Arct Antarct Alp Res 2010;42:98-105.
Ryker SJ. Mapping arsenic in groundwater. Geotimes 2001;46:34–6.
SNOTEL. National Resources Conservation Service; 2011. http://www.wcc.nrcs.usda.gov/snotel. Data accessed 22 March 2011.
Steenburgh WJ, Massey JD, Painter TH. Episodic dust events of Utah's Wasatch front and adjoining region. J Appl Meteor Climatol in press.
Thevenon F, Chiaradia M, Adatte T, Hueglin C, Pote J. Ancient versus modern mineral dust transported to high-altitude alpine glaciers evidences Saharan sources and atmospheric circulation changes. Atmos Chem Phys Discuss 2011;11:859–84.
Turk JT, Taylor HE, Ingersoll GP, Tonnessen KA, Clow DW, Mast MA, et al. Major-ion chemistry of the Rocky Mountain snowpack, USA. Atmos Environ 2001;35: 3957–66.
USEPA. The Clean Air Act Amendments of 1990 list of hazardous air pollutants; 1990. http://www.epa.gov/ttn/atw/orig189.html. Accessed 26 February 2012.
USEPA Method 1630. Methylmercury in water by distillation, aqueous ethylation, purge and trap, and CVAFS, January 2001; 38 pp.
USEPA Method 1631. Revision E. Mercury in water by oxidation, purge and trap, and cold vapor atomic fluorescence spectrometry, August 2002; 38 pp.
USEPA Method 1669. Sampling ambient water for trace metals at EPA water quality criteria levels, July 1996; 33 pp.
Veysseyre A, Moutard K, Ferrari C, Van de Velde K, Barbante C, Cozzi G, et al. Heavy metals in fresh snow collected at different altitudes in the Chamonix and Maurienne valleys, French Alps: initial results. Atmos Environ 2001;35:415–25.
Wedepohl KH. The composition of the continental crust. Geochim Cosmochim Acta 1995;59:1217–32.
Winiwarter W, Puxbaum H, Schoner W, Bohm R, Werner R, Vitovec W, et al. Concentration of ionic compounds in the wintertime deposition: results and trends from the Austrian Alps over 11 years (1983–1993). Atmos Environ 1998;32:4031–40.
Zoller WH, Gladney ES, Duce RA. Atmospheric concentrations and cources of trace metals at the South Pole. Science 1974;183:198–200.